

---

## Dissolved and particulate metals (Fe, Zn, Cu, Cd, Pb) in two habitats from an active hydrothermal field on the EPR at 13 degrees N

Pierre-Marie Sarradin<sup>a,\*</sup>, Delphine Lannuzel<sup>a</sup>, Matthieu Waeles<sup>b</sup>, Philippe Crassous<sup>a</sup>, Nadine Le Bris<sup>a</sup>, Jean Claude Caprais<sup>a</sup>, Yves Fouquet<sup>c</sup>, Marie Claire Fabri<sup>a</sup> and Ricardo Riso<sup>b</sup>

<sup>a</sup> Département Etudes des Ecosystèmes Profonds, Ifremer centre de Brest, BP70, F-29280 Plouzané, France

<sup>b</sup> Laboratoire de Chimie Marine, UBO et UMR CNRS 7144, Place Nicolas Copernic, F-29280 Plouzané, France

<sup>c</sup> Département Géosciences Marines, Ifremer centre de Brest, BP70, F-29280 Plouzané, France

\*: Corresponding author : P.M. Sarradin, email address : [Pierre.Marie.Sarradin@ifremer.fr](mailto:Pierre.Marie.Sarradin@ifremer.fr)

---

### Abstract:

The distribution of Fe, Cu, Zn, Pb, Cd between the dissolved (< 2 µm) and the particulate (> 2 µm) fractions was measured after in-situ filtration in two hydrothermal habitats. The total metal concentration ranges exhibit a clear enrichment compared with the seawater concentration, accounting for the hydrothermal input for all the metals considered. Iron is the predominant metal (5–50 µM) followed by Zn and Cu. Cd and Pb are present at the nM level. At the scale studied, the behavior of temperature, pH and dissolved iron is semi-conservative whereas the other dissolved and particulate metals are characterized by non-conservative patterns. The metal enrichment of the > 2 µm fraction results from the settlement and accumulation of particulate matter close to the organisms, acting as a secondary metal source. The enrichment observed in the dissolved fraction can be related to the dissolution or oxidation of particles (mainly polymetallic sulfide) or to the presence of small particles and large colloids not retained on the 2 µm frit. SEM observations indicate that the bulk particulate observed is characteristic of crystalline particles settling rapidly from the high temperature smoker (sphalerite, wurtzite and pyrite), amorphous structures and eroded particles formed in the external zone of the chimney. Precipitation of Zn, Cu, Cd and Pb with Fe as wurtzite, sphalerite and pyrite is the main process taking place within the area studied and is semi-quantitative. The distribution of the dominant observed fauna has been related to the gradient resulting from the dilution process, with the alvinellids worms colonizing the hotter and more variable part of the mixing zone, but also to the metallic load of the mixing zone. Dissolved and particulate metal concentrations are therefore necessary abiotic factors to be studied in a multiparametric approach to understand the faunal distribution in hydrothermal ecosystems.

**Keywords:** Metals; Dissolved; Particulate; Habitats; Hydrothermal fauna

---

### 1. Introduction

Deep-ocean hydrothermalism is the meeting point of deep-seated geological processes with the ocean above resulting in the transfer of heat and chemicals from the earth's deep mantle and the crust, through volcanic and hydrothermal systems. The physical and chemical characteristics of vent emissions are initially the result

1  
2 of complex rock seawater interactions in the subsurface that form high temperature hydrothermal fluids.  
3  
4 These fluids can be subsequently modified by seafloor and near surface mixing with background  
5 seawater leading to a variety of emitted fluids enriched with gases, metals and radionuclides (Bowers et al.,  
6 1985; Von Damm, 1988; 1998; Cherry et al., 1992).  
7

8  
9 Deep-sea hydrothermal communities occupy the interfacial zone where the hot and reduced hydrothermal  
10 fluid turbulently mixes with the cold and oxygenated seawater. The mixing zone is characterized by steep  
11 chemical gradients (Johnson et al., 1986; Sarradin et al., 1998; Le Bris et al., 2003) and produces mineral  
12 precipitation in the rising plume (Feely et al., 1990) or the chimney conduit (Metz and Trefry, 2000). This  
13 fluctuating environment provides a periodical access to reduced chemical species from the vent fluid (e.g.  
14 H<sub>2</sub>S, CH<sub>4</sub>) and seawater oxidized compounds which are both required for chemolithoautotrophic bacterial  
15 primary production and associated fauna (Childress and Fisher, 1992). Many authors have suggested links  
16 between the spatio-temporal distribution of hydrothermal species and the physical and chemical properties of  
17 the vent fluids: concentrations of hydrogen sulfide (Urcuyo et al., 2003), flow intensity and substratum type  
18 (Sarrazin et al., 1999), speciation and bioavailability of oxygen, iron and sulfur (Luther et al., 2001),  
19 particulate fluxes and variability in fluid composition (Desbruyères et al., 2000; 2001).  
20

21  
22 Hydrothermal species are also subjected to potentially toxic material, such as heavy metals, provided in large  
23 concentrations by the hydrothermal fluid (Douville et al., 2002). However, the main processes controlling the  
24 metal concentrations in these highly reactive areas and the influence of the metallic load of the mixing zone  
25 on species distribution have been poorly documented (Desbruyeres et al., 1998; Geret et al., 1998; 2002; Di  
26 meo-Savoie et al. 2004, Kadar et al., 2005). The main conclusion of ecotoxicological papers dealing with  
27 hydrothermal vent organisms (Cosson, 1996; Cosson-Manevy et al., 1988; Desbruyères et al., 1998; Ruelas-  
28 Inzunza et al., 2003) is the apparent contradiction between the large amounts of metals present in the  
29 organisms and the absence of recognizable deleterious effects. These organisms seem to have developed  
30 efficient adaptations and detoxification processes such as the sequestration of potentially toxic compounds  
31 into forms that are probably inactive: insoluble forms such as granules or concretions and soluble forms as  
32 metalloproteins (Cosson and Vivier, 1997; Geret et al, 2002). In consequence, there is a need to assess the  
33 metallic composition of these peculiar environments in order to understand its potential impact on the  
34 distribution of hydrothermal organisms and the efficiency of the detoxification processes involved.  
35

36  
37 This study was carried out at the Genesis hydrothermal vent field on the East Pacific Rise. Fe, Cu, Zn, Cd  
38 and Pb were analyzed in the environment surrounding hydrothermal organisms. Their distribution between  
39 the dissolved (<2µm) and particulate (>2µm) fractions is presented. The objectives were to document the  
40 content and behavior of these elements in this part of the mixing zone and to assess the potential link  
41 between the metallic load and the faunal distribution in two habitats dominated by alvinellids worms or giant  
42 tubeworms (*Riftia pachyptila*).  
43  
44  
45  
46  
47  
48  
49  
50  
51  
52  
53  
54  
55  
56  
57  
58  
59  
60  
61  
62  
63  
64  
65

## 2. Material and methods

### 2.1. The Genesis site (13°N, EPR)

This study was conducted during the HOPE 99 cruise on the East Pacific Rise (1999, N/O L'Atalante/submersible Nautille, Chief scientist F. Lallier) and focused on the Genesis vent field (12°48.63 N, 103°56.41W, depth 2645 m). This site is characterized by the presence of a black smoker emitting a medium temperature (230 – 290°C) hydrothermal fluid (Childress et al., 1993; Sarradin et al., 1998; Le Bris et al., 2003). The fluid may have undergone sub surface phase separation with a major contribution of vapor phase in the emitted fluid, enriched in CO<sub>2</sub>, depleted in iron (300 µM) and chloride (Le Bris et al., 2003) compared to the range previously established at 13°N (Von Damm, 1995a). The black smoker (Fig. 1) is 9 m high and is built on the 5 m upright wall oriented NW-SW bordering the western side of the Genesis hydrothermal vent field. The dominant species encountered in the vicinity of the smoker were *Riftia pachyptila* tubeworms and alvinellid worms such as *Alvinella pompejana*, *Alvinella caudata*, *Paralvinella grasslei* and *Hesiolyra bergi* (Desbruyères et al. 1998). *R. pachyptila* tubeworms live in an area (zone R) where the temperature ranges from 3 to 25°C (Sarradin et al., 1998; Le Bris et al., 2003). This area is a vertical crack on the 5 m upright wall a few meters north of the main chimney. Alvinellid worms were found in zone A (temperature 9 to 70°C) 5 meters north of the crack and 2 meters away from the bottom of the wall.

### 2.2. Sampling and sample treatment

Water samples were collected in the environment surrounding hydrothermal organisms. This environment is formed by the fluctuating mixing of cold seawater with hot hydrothermal fluid. Reference samples were taken at the periphery (c.a. 500 m) of the active area. The sampling device (Fig. 2) consisted of four 200 ml titanium bottles with an autonomous temperature probe (Micrel®) and manipulated by the manned submersible Nautille. The bottles were helium purged and set under vacuum (<2\*10<sup>2</sup> Pa) before use. Each sample inlet (PEEK tubing, 0.8 mm i.d.) was equipped with a PEEK polymer frit (UPCHURCH®, porosity 2 µm) to perform in-situ filtration of the sample. In-situ filtration should prevent/lower any modification of the sample by oxidation / reduction or precipitation phenomena with cooling. The frit porosity was set to 2 µm to overcome a potential explosion of the frit when opening the bottle with a pressure increase of c.a. 250 bars in a few msec. Titanium bottles, polymer frits and frit holders were rinsed with HCl 0.1M and ultrapure water before use. Subsamples devoted to the analysis of dissolved metal (~ 100 mL) were stored acidified (1/1000 V/V HNO<sub>3</sub>, Merck, suprapur) prior to on shore analysis. The 2 µm frits were dried for 24 h at 85°C and stored prior to on shore mineralization and analysis of the particulate fraction. The mineralization step was conducted in a 3 ml HCl 30% / 1 ml HNO<sub>3</sub> 65% / 1 ml HF 40 % mixture by heating for 3 hours at 80°C and 1 hour at 100°C. The volume of the obtained solution was corrected by weighing to take into account the loss during the mineralization step. Subsamples were analyzed after dilution in 2% HNO<sub>3</sub> (ICP-MS) or suprapure water (Potentiometric Stripping Analysis).

### 2.3. Analytical methods

pH of the samples was measured on board after submersible recovery using a combined pH electrode (Ingold®) for a sulfide rich medium. Measurements were made at 25°C after calibration with NBS buffers (pH 4 and 7). Sample temperatures were derived from the data recorded by the autonomous temperature probe associated with the sample inlet. Fe concentrations were determined by Flow Injection Analysis according to the procedure detailed in Sarradin et al. (2005). Reproducibility and detection limits are 0.8 % (n=5, 50 µM) and 70 nM respectively. Cu, Pb and Cd levels were measured by using electrochemical methods. Cu measurement was performed by Constant Current Stripping Chronopotentiometry (CCSA) with a gold electrode. Pb and Cd were measured by Potentiometric Stripping Analysis (PSA) with a mercury film electrode. Reproducibilities are 2, 5 and 4% for Cu, Pb and Cd, detection limits are respectively 0.17, 0.01 and 0.01 nM. The procedures has been detailed in Riso et al. (1997a, 1997b) and one of their assets is that they need no UV irradiation to get the total dissolved metal concentrations. Certified sea waters were analysed for metal content prior to the samples (Table 1). Zn concentrations were determined by ICP-MS (Université de La Rochelle, Centre Commun d'Analyses, Varian Ultramass 700). The ICP-MS system operated in peak hopping mode with a dwell time of 40 ms per isotope. Instrumental conditions were: plasma power 1250 W, plasma flow 15 L/min, auxiliary plasma 1.50 L/min, nebulizer flow 0.90 L/min, 15 scans/replicate, 10 replicates/sample. The instrument was calibrated using commercially available aqueous standard solution (Astasol-Mix, Analytika Ltd, purity 99.999%). The quantification was done using the standard addition method to overcome the potential matrix effect. Three internal standards (Y, Rh, Eu) were also added to the samples to validate the results. Reproducibility and detection limits are 4% and 0.15 nM respectively. All reagents were prepared in a clean room.

In order to check whether the samples were free from contamination during sampling and handling, 2 samples were taken ca. 500 m away from the active area. The concentrations of dissolved metals obtained in sample SW1 (Fe < detection limit, Cu 0.01µM, Cd 1.3 nM, Pb 1.5 nM) are close to those currently reported for North Pacific deep waters (Fe 0.01 µM, Cu 0.005µM, Cd 1 nM, Pb 0.005 nM, Donat and Bruland, 1995) except for Pb. The values obtained in sample SW2 are relatively higher (Fe 1.9 µM, Cu 0.02µM, Cd 1.1 nM, Pb 1.5 nM) and can be linked to an input of hydrothermal material or to a limited contamination problem for lead. However, these levels remain below those found in the samples taken in the immediate surrounding of hydrothermal communities which were measured at the following ranges Fe: 1-33 µM, Cu 0.17-1.13 µM, Cd 1.8-8.56 nM, Pb 10.3-61.9 nM.

### 2.4. Scanning Electronic Microscope analysis and particle characterization

To determine the raw composition and the morphology of minerals on the particle samples, a Philips XL30 scanning electron microscope (SEM) equipped with an EDAX® detector was used at energy of 15 kV. The frits were gold coated prior to their analysis (Balzers® SCD 040). The characterization of the particulate matter was conducted on 2 frits (corresponding to samples R3, T= 4.3°C and A4, T=12.8°C). These 2 samples were supposed to give us a snapshot of the minerals present in the cold and warm part of the mixing zone. In the first stage, 6 analyses were performed on a frit transect at low magnification to establish the raw

1  
2  
3 composition of the particles and to evaluate the homogeneity of the samples. The second stage was  
4 conducted at higher magnification in order to recognize and list the dominant mineral structures and to  
5 establish their elemental composition. Elemental analysis was done using the EDAX<sup>®</sup> detector and was  
6 followed by a visual recognition of the structures (Y. Fouquet).  
7  
8  
9

#### 10 2.4. Statistical methods

11 Statistical treatments were done using the Statgraphics Plus 5.1 software. Principal components analysis  
12 (PCA) is a technique used to reduce multidimensional data sets to lower dimensions for analysis. PCA is  
13 mostly used as a tool in exploratory data analysis. A study of the rank correlation (Spearman) was performed  
14 prior the PCA to identify the independent variables.  
15  
16  
17  
18  
19

### 20 3. Results and discussion

#### 21 3.1. Temperature and pH

22  
23 Temperature and pH measurements are shown in table 2. The samples were collected in the cold part of the  
24 mixing zone with temperature and pH ranging from 3.8 to 20°C and 7.1 to 5.9, respectively. The  
25 corresponding hydrothermal input estimated from the endmember concentrations is limited to 0.6 to 7.9%.  
26 The environment of the dominant species colonizing the Genesis vent site is thus not fully represented as the  
27 hot part of the mixing zone, preferred habitat of Alvinellid worms, with measured temperature up to 70 or  
28 80°C (Sarradin et al., 1998; Le Bris et al., 2003; Di Meo-Savoie et al., 2004), has not been effectively  
29 sampled. However, the samples obtained (Fig. 3a) cover the whole temperature range encountered by the  
30 giant tubeworms *Riftia pachyptila* and the colder part of the microhabitat of Alvinellids as can be seen in Fig.  
31 3b. Fig. 3b was obtained using temperature time series measured by autonomous probes (Micrel®) during 2  
32 cruises on the EPR (HOT96 and HOPE99, n = 10478, unpublished data).  
33  
34  
35  
36  
37  
38  
39  
40  
41

#### 42 3.2. Fe, Zn, Cu, Cd and Pb concentrations

43 Total metal concentration ranges obtained are presented in table 3 along with those reported for other studies  
44 in environments surrounding hydrothermal organisms. Fe is the predominant element with concentrations in  
45 the range 5-63 µM. Cu and Zn exhibit levels varying from 0.18 to 1.6 µM and from 0.3 to 27.3 µM,  
46 respectively. Cd and Pb were measured at the nM level with values in the range 2-47 and 11-260,  
47 respectively. All these concentrations are well above those reported for deep North Atlantic waters (Donat  
48 and Bruland, 1995) illustrating a marked metallic enrichment due to hydrothermal inputs. The ranges  
49 obtained are comparable though lower than those presented by Desbruyères et al. (1998) in the same area  
50 and by Di Meo-Savoie et al. (2004) at 9°N. These two studies were performed in the hot part of the mixing  
51 zone colonized by *Alvinella pompejana*. Compared to the studies carried out on the colder habitats of the  
52 hydrothermal mussels *Bathymodiolus azoricus* and the shrimps *Rimicaris exoculata* on the mid Atlantic  
53 Ridge (Geret et al., 1998; 2002; Sarradin et al., 1999; Kadar et al., 2005), the ranges were again similar. High  
54 metallic concentrations were encountered around hydrothermal organisms, bearing in mind the heterogeneity  
55  
56  
57  
58  
59  
60  
61  
62  
63  
64  
65

1  
2  
3 of the mixing zone and the chemical diversity of hydrothermal fluids (Von Damm, 1995a). The comparison  
4 between the dissolved ( $<2\ \mu\text{m}$ ) and particulate ( $>2\ \mu\text{m}$ ) fractions indicates that Zn, Fe and Cd are mainly  
5 associated with particles whereas Cu and Pb are roughly equally distributed between both fractions. The use  
6 of a  $0.45\text{-}\mu\text{m}$  filters should enhance the importance of the particulate fraction by incorporating the small  
7 particles and large colloids not retained on the  $2\ \mu\text{m}$  frits.  
8  
9

### 10 *3.3. Metal behavior in the mixing zone*

11 The possibility of using temperature or pH as dilution tracer of hydrothermal fluid by seawater (Le Bris et  
12 al., 2000) was tested using the T/pH relationship of our samples enriched by published data from Von Damm  
13 (1995a) and Le Bris et al. (2003) obtained at the same site. The linear trend obtained (confidence level 99%,  
14 Fig. 4) can explain 96% of the variability in the data. This result confirms that at the scale and in the range  
15 studied, pH and temperature can be assumed to follow a semi-conservative process and can be used as  
16 tracers of the dilution, even though conductive cooling in the subsurface can modify its conservative  
17 behavior during mixing.  
18  
19

20 The amount of dilution of hydrothermal fluid by seawater in the samples (table 2) was derived from this  
21 conservative behavior and by using the data published by Le Bris et al. (2003). Assuming a seawater  
22 temperature of  $1.9^\circ\text{C}$  with no hydrothermal input and a pure fluid temperature in Genesis of  $230^\circ\text{C}$  (Le Bris  
23 et al. 2003), the amount of hydrothermal fluid in the mixture was estimated as being % fluid = (Temperature  
24  $-1.9)/2.281$ .  
25  
26

27 In order to check whether the concentrations of the metals studied in the mixing zone are controlled by a  
28 dilution-like process, dissolved and particulate metal concentrations were plotted against temperature (Fig.  
29 5). Theoretical dilution lines were estimated using the two components of the mixture i.e. the concentrations  
30 and temperature of the pure fluid and seawater presented in Table 3. No endmember value was available for  
31 Cu. The endmember Fe concentration was taken at  $300\ \mu\text{M}$ , most recent value obtained by Le Bris et al.  
32 (2003) for this particular vent field.  
33  
34

35 No trends were observed between metal concentrations and temperature except for dissolved iron. Fe  
36 presents a weak but significant relationship with temperature (confidence level 95%) explaining only 30% of  
37 the variability. This lack of relationship between metal concentrations and temperature indicates that both  
38 dissolved and particulate forms are not controlled by a simple dilution process at the scale studied. By  
39 comparing the values obtained with the theoretical dilution line (Fig. 5), it can be noted that particulate metal  
40 concentrations are mainly located above the dilution line suggesting the presence of a secondary metal input.  
41 This enrichment, which is particularly important for all the metals studied, should result from the continuous  
42 settlement and accumulation of particulate matter close to the organisms. These observations are supported  
43 by the ability of Cu, Fe, Zn, Cd and Pb to form precipitates with sulfides in plumes, chimney or in conduits  
44 surfaces (Trefry and Trocine, 1985; Von Damm et al., 1995b). Iron will form preferentially fine grained  
45 sulfides particles that will be exported in the buoyant and neutrally buoyant plume. Cu and Zn sulfides will  
46 form large sized grains and more crystalline particles that will settle rapidly in the near field region (Feely et  
47 al., 1994). In the dissolved ( $<2\ \mu\text{m}$ ) fraction, enrichments observed for Cd and Pb can be explained by the  
48 presence of small particles or large colloids not retained on the  $2\ \mu\text{m}$  filter. The particles accumulated  
49  
50  
51  
52  
53  
54  
55  
56  
57  
58  
59  
60  
61  
62  
63  
64  
65

1  
2  
3 (mainly polymetallic sulfides) may also undergo dissolution and/or oxidation reaction in this cold part of the  
4 mixing zone which contains dissolved oxygen (Dunk and Mills, 2006). On the contrary, dissolved Fe and Zn  
5 are close to or below the theoretical dilution line as observed by Di Meo et al. (2004). This depletion should  
6 correspond to the precipitation of Fe and Zn sulfides (Di Meo et al. 2004, Luther et al. 2001). Sander et al.  
7 (2007) also evidenced the presence of organic ligands that will form strong complexes likely to play an  
8 important role in controlling the behavior of metal ions around hydrothermal vents.  
9

### 10 11 12 13 14 *3.4. Particle characterization and origin*

15 Observations by SEM permitted the determination the elemental composition of particles and the  
16 investigation of their origin. Measurements indicated that the dominant elements were sulfur ( $26.2 \pm 3$  %),  
17 zinc ( $19.7 \pm 2.2$  %), iron ( $16.5 \pm 3$  %), sodium ( $7.1 \pm 3.7$  %), chloride ( $5.3 \pm 1.4$  %) and silica ( $7.7 \pm 1.6$  %).  
18 The presence of residual NaCl can be explained by an incomplete rinsing of the frits before analysis. These  
19 compositions can be compared to the data obtained by German et al. (2002) within the Totem site (EPR,  
20  $13^\circ\text{N}$ ) on particles sampled with traps a few meters from the vent. These authors found higher S composition  
21 (50 to 80%) and comparable Fe one (11-20%). The Fe/S, Zn/S and Fe/Zn atomic ratio obtained in this study  
22 are respectively 0.4, 0.4 and 1, leading to a relative stoichiometry of  $\text{FeZnS}_{2.5}$ . The mean composition of the  
23 particles was homogeneous along frit transects permitting the second stage of particle identification to be  
24 performed at a higher magnification. Table 4 lists the dominant structures observed and summarizes 32  
25 individual observations (Y. Fouquet). No obvious difference was observed between the 2 frits studied. The  
26 particles were predominantly zinc – iron sulfides (wurtzite and sphalerite) and iron sulfides (pyrite). The  
27 minerals were present in their crystalline form, with large individual crystals (up to  $50\mu\text{m}$ ) and smaller  
28 crystals (1 to  $5\mu\text{m}$ ) forming stacks reaching up to  $20\mu\text{m}$ . These crystalline structures were probably formed  
29 in an area where the chemical conditions are homogeneous, *i.e.* in the internal part of the chimney. The  
30 amorphous forms were also frequent. These forms should originate from precipitation in the external part of  
31 the chimney (cold part of the mixing zone, chimney walls). The presence of microcrystalline structures  
32 associated with a biofilm-like substance was nearly ubiquitous. This organic material could either be  
33 exopolysaccharids (J. Guezennec, com. pers.) or mucous excreted by organisms such as alvinellid worms.  
34 Laboratory experiments conducted by Loaec et al. (1997, 1998) reported the biosorption of lead, cadmium  
35 and zinc by an exopolysaccharid produced by hydrothermal strains through a chemical equilibrated and  
36 saturable mechanism. The presence of exopolysaccharids has to be verified as this organic material enriched  
37 in metals could be directly assimilated by organisms through dietary exposure. Particulate matter such as  
38 anhydrite which is a dominant constituent of the plume was seldom observed. The rare observation of  
39 anhydrite and the absence of observation of iron oxyhydroxide phases suggest that the plume has only a  
40 limited impact on the environment surrounding hydrothermal communities (Mottl and MacConachy, 1990).  
41 Zbinden et al. (2003) observed the presence of sphalerite, wurtzite, pyrite and marcasite minerals as major  
42 constituents of the solid phase associated with alvinellid tubes. These observations are strengthened by the  
43 statement of German et al. (2002). These authors indicated that sulfides particles carry 80-90% of the Fe fall  
44 out and also transport most of the Cu, Zn and Pb fluxes, whereas Fe oxyhydroxides were responsible for only  
45  
46  
47  
48  
49  
50  
51  
52  
53  
54  
55  
56  
57  
58  
59  
60  
61  
62  
63  
64  
65

1  
2  
3 10-20 % of the Fe removal. Furthermore, the composition of vent particles in southern Juan de Fuca (Feely  
4 et al., 1987) was predominately sphalerite, wurtzite and pyrite whereas suspended and settling particles 100  
5 m away from the vent were mainly sphalerite, anhydrite and Fe oxyhydroxide. The bulk particulate observed  
6 in our samples is composed of particles formed in the high temperature smoker which settle rapidly  
7 (sphalerite, wurtzite and pyrite) and of amorphous structures and eroded particles coming from external  
8 zones of the chimney. This last observation reinforces the hypothesis of particle accumulation in areas where  
9 hydrothermal organisms have settled.

10  
11 According to Trocine and Trefy (1988) and German et al. (1991), we used particulate iron concentrations  
12 (Fep) as an indicator of the trends and factors influencing other particulate metals. High positive linear  
13 correlations (confidence level 99%, correlation coefficient ranging from 0.918 to 0.972) were obtained  
14 between particulate Cu, Zn, Cd, Pb vs. Fep (Fig. 6). These correlations can explain between 84 to 94 % of  
15 the variability observed in the data and indicate that Zn, Cu, Cd and Pb will co-precipitate with Fe as  
16 wurtzite, sphalerite and pyrite. Moreover, this high correlation underlines that this precipitation is the main  
17 process involved within the studied area and is nearly quantitative. Mottl and MacConachy (1990) also stated  
18 that the chalcophile elements released into the water column from vent fluids tend to be quantitatively  
19 removed from solution very close to their point of origin through precipitation with Fe as polymetallic  
20 sulfides. In the same way, Cd and Pb will be associated as trace elements, during the precipitation step to  
21 form Zn-Fe sulfides in the wurtzite and sphalerite phases precipitated below 200°C (Trocine and Trefy,  
22 1988; Metz and Trefry, 2000).

### 34 *3.5. Metallic load and faunal distribution*

35  
36 The data were submitted to Principal Component Analysis, a statistical exploratory method to highlight the  
37 links between the whole set of variables. Study of the rank correlation (Spearman) allowed the identification  
38 of the independent variables. Significant correlations were found at the 95% level i) between dissolved Cu,  
39 Cd and Pb, ii) between all the particulate concentrations as stated above (see 3-4) and iii) between pH and  
40 temperature (see 3-2). The remaining variables to be used for the PCA were temperature (T°C correlated  
41 with pH), dissolved iron (Fed), zinc (Znd) and cadmium (Cdd correlated with Cud and Pbd) and particulate  
42 iron (Fep correlated with all the particulate metals). Two components explaining 72% of the variability of the  
43 data were extracted by the analysis and are presented in Fig. 7. The use of a third axis explained 15% more  
44 of the variability but did not add new information. The first axis opposes the variables temperature (T°C) and  
45 dissolved iron (with respective coordinates on the correlation circle of -0.60 and -0.57) to the 3 other  
46 variables Cdd, Znd, Fep (with respective coordinates of 0.42, 0.29, 0.22). The second axis essentially  
47 confronts particulate iron (0.51 on the correlation circle) to dissolved Zn and Cd (-0.58 and -0.53 on the  
48 correlation circle) and temperature and dissolved Fe (0.22 and 0.25). The combination of the 2 axes  
49 illustrates the complexity of processes occurring in the mixing zone. T°C and Fed are linked to a dilution  
50 process between the cold seawater and the hot fluid. Particulate (>2µm) metal concentrations result from the  
51 precipitation and accumulation of polymetallic sulfides. The other dissolved metals (<2 µm) have different  
52  
53  
54  
55  
56  
57  
58  
59  
60  
61  
62  
63  
64  
65

1  
2 behaviors and include the processes that may occur within the 0.45 – 2  $\mu\text{m}$  phase constituted of small  
3 particles and large colloids.  
4

5 A projection of the observations on the biplots highlights their position along the two axes as a function of  
6 the sampling zone. Samples obtained in areas dominated by the tubeworm *R. pachyptila* (R) are  
7 characterized by a limited variability along the 2 components corresponding to the cold part of the mixing  
8 zone (Childress et al., 1993; Sarradin et al., 1998; Le Bris et al., 2003). Samples collected in areas dominated  
9 by alvinellid worms (A) showed a higher variability associated with extreme values along the 2 axis (A1  
10 16°C, Fed 33.7 $\mu\text{M}$ ; A5 Zn 2 $\mu\text{M}$ , Cd 7.84nM; A6 Fe 57.1 $\mu\text{M}$ ). The microhabitat of alvinellid worms  
11 present steeper gradients but is not fully represented in our study. Faunal assemblages dominated by  
12 alvinellids are present in a temperature range between 9.6-81°C (Desbruyères et al., 1998; Le Bris et al.,  
13 2003; 2005; Sarradin et al., 1998; Di Meo-Savoie et al., 2004). The temperature range and therefore the  
14 fraction of the mixing zone sampled in this study is only 3.2 to 20°C, leaving the hot part of the mixing zone  
15 unsampled, even though *A. pompejana* has developed a specific strategy to cool and modify the fluid mixture  
16 within its tube (Le Bris et al. 2005).  
17

18 The faunal distribution in hydrothermal environment has been shown to depend upon fluid dilution process,  
19 sulfide concentrations and speciation (Luther et al., 2001, Le Bris et al., 2003), flow intensity or substratum  
20 type (Sarrazin et al., 1999). From this multiparametric descriptive analysis, it can be hypothesized that the  
21 distribution of the observed dominant fauna is not only constrained by these variables, but also by the  
22 concentration and speciation of metals which are controlled by complex geochemical processes.  
23 Hydrothermal organisms will therefore colonize areas where the energy supply ( $\text{H}_2\text{S}$  and  $\text{CH}_4$ , flow  
24 intensity) is sufficient, where the substratum is convenient but also where the environment is suitable i.e.  
25 where the metals bioavailability can be sustained. This result is particularly important in this area where the  
26 two dominant species present different nutritional strategies and hence different sensitivity to dissolved and  
27 particulate metals. *Alvinella pompejana* (Desbruyères et al., 1998) is a grazer (particulate feeding consumer).  
28 This organism will ingest large quantities of metal rich particulate matter (Cosson and Vivier, 1997) that may  
29 serve as the main pathway for metal accumulation. Wang (2002) suggested that the metal desorption within  
30 the acidic gut may be important for the assimilation of easily exchangeable metals but not for metals that are  
31 bound tightly. Zbinden et al. (2003) observed the presence of mineral gradients between the inner and outer  
32 part of the alvinellids' tubes suggesting that the tube wall acts as an efficient barrier to external environment,  
33 including metal compounds. Conversely, *Riftia pachyptila* is a symbiotic tubeworm devoid of mouth and gut  
34 that will transfer hydrogen sulfide to its symbiotic bacteria harbored in the trophosome (Goffredi et al.,  
35 1997). The majority of the exchange of this organism with its environment will take place through the  
36 branchial plume: the metal entry route will be either by adsorption of the particles on the membrane or by  
37 direct crossing of the membrane by the dissolved fraction i.e. with no direct impact of metallic particles. Cu,  
38 Cd, Zn have been quantified in the blood and can be transported from the plume to the trophosome (Cosson-  
39 Manevy et al., 1988) yet with limited metallic bioaccumulations in the bacteria present in the trophosome  
40 (Truchet et al., 1998). Ruelas-Inzunza et al. (2005) observed that Cd and Fe concentrations in the  
41 vestimentum increased accordingly with the size of specimens and reported an extreme uptake in the case of  
42  
43  
44  
45  
46  
47  
48  
49  
50  
51  
52  
53  
54  
55  
56  
57  
58  
59  
60  
61  
62  
63  
64  
65

1  
2  
3 Cu and Zn. The metal compounds will be stored in the tissues as non toxic mineral compounds or associated  
4 to metallothioneins known to be involved in detoxication processes (Cosson, 1996).

5  
6 Riftia clumps are present in zone R characterized by a limited variability, low temperature and metal  
7 concentrations whereas Alvinellids worms in zone A are exposed to stronger metal gradients and fluctuations  
8 than the tubeworms. This distribution along the chemical gradient can be linked both to the availability of  
9 energy sources but also to the ability of *Riftia pachyptila* or alvinellids worms to sustain the metallic load,  
10 alvinellids being potentially more adapted to tolerate harsher conditions. The possible metal entry routes may  
11 also be different as only the dissolved metal fraction will be available for *R. pachyptila*, whereas both  
12 dissolved and particulate fractions will be available for alvinellid worms. The role of metal speciation on  
13 bioavailability and toxicity towards the different faunal species has to be evaluated to examine if the metallic  
14 load is a key factor to explain faunal distribution in hydrothermal ecosystems.  
15  
16  
17  
18  
19  
20

#### 21 **4. Conclusion**

22  
23 This study tentatively describes the complexity of the hydrothermal biotope regarding the metal input and the  
24 relative distribution of Fe, Cu, Zn, Cd and Pb between a dissolved (<2 $\mu$ m) and particulate (>2  $\mu$ m) fraction.

25  
26 The total metal concentration ranges exhibit a neat metallic enrichment accounting for the hydrothermal  
27 input of this part of the mixing zone for all the metals considered compared with the seawater concentration.

28  
29 At the scale studied, temperature, pH and dissolved iron have a (semi-) conservative behavior whereas the  
30 other dissolved metals and the particulate metals are characterized by non-conservative behaviors involving  
31 different processes. The metal enrichment of the particulate fraction results from the settlement and  
32 accumulation of particulate matter close to the organisms. This accumulation can be seen as a significant  
33 secondary source of particulate metals. The enrichment observed in the dissolved fraction can be induced by  
34 the dissolution and/or oxidation of particles (mainly polymetallic sulfide) or by the presence of particles or  
35 colloids which size ranges from 0.45 to 2  $\mu$ m.  
36  
37  
38  
39

40  
41 The bulk particulate observed in our samples is characteristic of crystalline particles settling rapidly from the  
42 high temperature smoker (sphalerite, wurtzite and pyrite), amorphous structures and eroded particles formed  
43 in the external zone of the chimney. This observation reinforces the hypothesis of particle accumulation in  
44 areas where hydrothermal organisms have settled. Precipitation of Zn, Cu, Cd and Pb with Fe as wurtzite,  
45 sphalerite and pyrite is the main process involved within the studied area for the particles larger than 2 $\mu$ m.  
46

47  
48 The distribution of the observed dominant fauna can be related not only to the gradient resulting from the  
49 dilution process and hence the availability of energy sources but also to the metallic load and variability of  
50 the mixing zone. Distribution between dissolved and particulate fractions of the metals can be a first key to  
51 estimate metal bioavailability for organisms using different nutritional strategies such as *R. pachyptila* and  
52 alvinellid worms. Dissolved and particulate metal concentrations are therefore necessary abiotic variables in  
53 understanding the chemical reactivity of the environment. The study of faunal distribution in hydrothermal  
54 ecosystem should therefore be undertaken by a multiparametric approach taking into account both the  
55 necessary compounds available (O<sub>2</sub>, H<sub>2</sub>S, ...) but also the potential stressors such as metals present in this  
56  
57  
58  
59  
60  
61  
62  
63  
64  
65

1  
2 peculiar environment. The bioavailability of the metal compounds towards the different faunal species has to  
3 be evaluated to understand the strategies developed by hydrothermal fauna to cope with this environment.  
4  
5  
6

#### 7 **Acknowledgements**

8  
9 The authors are grateful to the N/O L'Atalante and deep submersible Nautille crew and to F. Lallier, scientific  
10 leader of the HOPE99 cruise for their assistance. Special appreciation goes to P. Rodier and P. Briand for  
11 their technical support, and Michel Robert (Univ. La Rochelle). This work was done with the financial  
12 support of MAST III project AMORES (MAS3-CT95-0040), 5<sup>th</sup> PCRD project VENTOX (EVK3-1999-  
13 00016) and the ANR-06-BDIV-005 DEEP OASES. We would like to thank David Banks, Professor of  
14 English Linguistics at the Université de Bretagne Occidentale, and the two reviewers for their useful  
15 comments on this article.  
16  
17  
18  
19  
20

#### 21 **References**

- 22  
23  
24 Bowers TS, Von Damm KL, Edmond JE. Chemical evolution of mid-ocean ridge hot springs. *Geochim*  
25 *Cosmochim Acta* 1985;2239-2252.  
26  
27 Cherry R, Desbruyères D, Heyraud M, Nolan C. High levels of natural radioactivity in hydrothermal vent  
28 polychaetes. *Comptes Rendus Aca Sci* 1992;série III:21-26.  
29  
30 Childress JJ, Fisher CR. The biology of hydrothermal vent animals: physiology, biochemistry and autotrophic  
31 symbioses. *Oceanography and Marine Biology Annual Review*. M Barnes, AD Ansell, RN Gibson (Eds),  
32 UCL press 1992;30:337-441.  
33  
34 Childress JJ, Lee RW, Saunders NK, Felbeck H, Oros DR, Toulmond A, Desbruyères D, Kennicutt MC, Brooks J.  
35 Inorganic carbon uptake in hydrothermal vent tubeworms facilitated by high environmental pCO<sub>2</sub>. *Nature*  
36 1993;11 March:147-149.  
37  
38 Cosson-Manevy MA, Cosson RP, Gaill F, Laubier L. Transfert, accumulation et régulation des éléments minéraux  
39 chez les organismes des sources hydrothermales. *Oceanol Acta* 1988;219-226.  
40  
41 Cosson RP. La bioaccumulation des éléments minéraux chez le vestimentifère *Riftia pachyptila* (Jones): bilan des  
42 connaissances. *Oceanol Acta* 1996;n°2:163-176.  
43  
44 Cosson RP, Vivier JP. Interactions of metallic elements and organisms within hydrothermal vents. *Cah Biol Mar*  
45 1997;43-50.  
46  
47 Desbruyères D, Chevaldonne P, Alayse-Danet AM, Caprais JC, Cosson R, Gaill F, Guezennec J, Hourdez S,  
48 Jollivet D, Jouin-Toulmond C, Lallier FH, Laubier L, Riso R, Sarradin PM, Toulmond A, Zal F. Burning  
49 subjects: biology and ecology of the "Pompei worm" (*Alvinella pompejana* Desbruyères et Laubier), a  
50 normal dweller of an extreme deep-sea environment. *Deep Sea Res II* 1998;383-422.  
51  
52 Desbruyères D, Almeida A, Biscoito M, Comtet T, Khripounoff A, Le Bris N, Sarradin PM, Segonzac M. A review  
53 of the distribution of hydrothermal vent communities along the Northern Mid Atlantic Ridge: Dispersal vs  
54 environmental controls. *Hydrobiol* 2000;201-216.  
55  
56  
57  
58  
59  
60  
61  
62  
63  
64  
65

- 1  
2  
3 Desbruyères D, Biscoito M, Caprais JC, Colaço A, Comtet T, Crassous P, Fouquet Y, Khripounoff A, Le Bris N,  
4 Olu K, Riso R, Sarradin PM, Segonzac M, Vangriesheim A. Variations in deep-sea hydrothermal vent  
5 communities on the Mid-Atlantic ridge near the Azores plateau. *Deep Sea Res I* 2001;1325-1346.  
6  
7 Di Meo-Savoie CA, Luther I, George W, Cary SC. Physicochemical characterization of the microhabitat of the  
8 epibionts associated with *Alvinella pompejana*, a hydrothermal vent annelid. *Geochim Cosmochim Acta*  
9 2004;9:2055-2066.  
10  
11 Donat JR, Bruland KW. Trace elements in the oceans, Chap. 11. Trace elements in natural waters. E Steinnes, B  
12 Saldo (Eds). Boca Raton, FLA, CRC Press 1995;302.  
13  
14 Douville E, Charlou JL, Oelkers EH, Biennu P, Colon CFJ, Donval JP, Fouquet Y, Prieur D, Appriou P. The  
15 Rainbow vent fluids (36°14'N, MAR): the influence of ultramafic rocks and phase separation on trace metal  
16 content in Mid-Atlantic Ridge hydrothermal fluids. *Chem Geol* 2002;1-2:37-48.  
17  
18 Dunk R, Mills RA. The impact of oxic alteration on plume-derived transition metals in ridge flank sediments from  
19 the East Pacific Rise. *Mar Geol* 2006;229:133-157.  
20  
21 Feely RA, Lewison M, Massoth GJ, Robert-Baldo G, Lavelle JW, Byrne RH, Von Damm KL, Curl Jr HC.  
22 Composition and dissolution of black smoker particulates from active vents on the Juan de Fuca Ridge. *J*  
23 *Geophys Res* 1987;B11:347-363.  
24  
25 Feely RA, Geiselman TL, Baker ET, Massoth GJ, Hammond SR. Distribution and composition of hydrothermal  
26 plumes particles from the ASHES vent field at axial volcano, Juan de Fuca ridge. *J Geophys Res*  
27 1990;B8:12855-12873.  
28  
29 Feely RA, Gendron JF, Baker ET, Lebon GT. Hydrothermal plumes along the East Pacific Rise, 8°40 to 11°50 N:  
30 Particle distribution and composition. *Earth Planet Sci Lett* 1994;19-36.  
31  
32 Geret F, Rouse N, Riso R, Sarradin PM, Cosson RP. Metal compartmentalization and metallothionein isoforms in  
33 mussels from the Mid-Atlantic Ridge; preliminary approach to the fluid-organism relationship. *Cah Biol Mar*  
34 1998;291-293.  
35  
36 Geret F, Riso R, Sarradin PM, Caprais JC, Cosson RP. Metal bioaccumulation and storage forms in the shrimp,  
37 *Rimicaris exoculata*, from the Rainbow hydrothermal field (Mid Atlantic Ridge); preliminary approach to  
38 the fluid-organism relationship. *Cah Biol Mar* 2002;43-52.  
39  
40 German CR, Campbell AC, Edmond JM. Hydrothermal scavenging at the Mid Atlantic Ridge: modification of  
41 trace element dissolved fluxes. *Earth Planet Sci Lett* 1991;101-114.  
42  
43 German C, Colley S, Palmer MR, Khripounoff A, Klinkhammer GP. Hydrothermal plume-particle fluxes at 13°N  
44 on the East Pacific Rise. *Deep Sea Res I* 2002;1921-1940.  
45  
46 Goffredi SK, Childress JJ, Desaulniers NT, Lallier FH. Sulfide acquisition by the vent worm *Riftia pachyptila*  
47 appears to be via uptake of HS<sup>-</sup> rather than H<sub>2</sub>S. *J Exp Biol* 1997;2609-2616.  
48  
49 Johnson KS, Beelher CL, Sakamoto-Arnold CM, Childress JJ. In situ measurements of chemical distributions in a  
50 deep-sea hydrothermal vent field. *Science* 1986;7 March:1139-1141.  
51  
52 Kadar E, Costa V, Martins I, Serrao Santos R, Powell J. Enrichment in trace metals (Al, Mn, Co, Cu, Mo, Cd, Fe,  
53 Zn, Pb and Hg) of macro-invertebrate habitats at hydrothermal vents along the Mid-Atlantic Ridge.  
54 *Hydrobiol* 2005;548:191-205.  
55  
56  
57  
58  
59  
60  
61  
62  
63  
64  
65

- 1  
2  
3 Le Bris N, Sarradin P, Birot D, Alayse-Danet A. A new chemical analyzer for in situ measurement of nitrate and  
4 total sulfide over hydrothermal vent biological communities. *Mar Chem* 2000;1:1-15.  
5  
6 Le Bris N, Sarradin PM, Caprais JC. Contrasted sulphide chemistries in the environment of 13°N EPR vent fauna.  
7 *Deep Sea Res I* 2003;6:737-747.  
8  
9 Le Bris N, Zbinden M, Gaill F. Processes controlling the physico-chemical micro-environments associated with  
10 Pompeii worms. *Deep Sea Res I* 2005;6:1071-1083.  
11  
12 Loaec M, Olier R, Guezennec J. Uptake of lead, cadmium and zinc by a novel bacterial exopolysaccharide. *Wat*  
13 *Res* 1997;5:1171-1179.  
14  
15 Loaec M, Olier R, Guezennec J. Chelating properties of bacterial exopolysaccharides from deep-sea hydrothermal  
16 vents. *Carbohydrate Polymers* 1998;65-70.  
17  
18 Luther GW, Rozan TF, Taillefert M, Nuzzio DB, Di-Meo C, Shank TM, Lutz RA, Cary SC. Chemical speciation  
19 drives hydrothermal vent ecology. *Nature* 2001;12 April:813-816.  
20  
21 Metz S, Trefry JH. Chemical and mineralogical influences on concentrations of trace metals in hydrothermal fluids.  
22 *Geochim Cosmochim Acta* 2000;13:2267-2279.  
23  
24 Mottl MJ, MacConachy TF. Chemical processes in buoyant plumes on the EPR near 21 N. *Geochim Cosmochim*  
25 *Acta* 1990;1911-1927.  
26  
27 Riso RD, Le Corre P, Chaumery CJ. Rapid and simultaneous analysis of trace metals (Cu, Pb, and Cd) in seawater  
28 by potentiometric stripping analysis. *Anal Chim Acta* 1997a;83-89.  
29  
30 Riso RD, Monbet P, Le Corre P. Measurement of copper in sea-water by constant current stripping analysis  
31 (CCSA) with a rotating gold disk electrode. *Analyst* 1997b;1593-1596.  
32  
33 Ruelas-Inzunza J, Soto LA, Paez-Osuna F. Heavy-metal accumulation in the hydrothermal vent clam *Vesicomya*  
34 *gigas* from Guaymas basin, Gulf of California. *Deep Sea Res I* 2003;757-761.  
35  
36 Ruelas-Inzunza J, Paez-Osuna F, Soto LA. Bioaccumulation of Cd, Co, Cr, Cu, Fe, Hg, Mn, Ni, Pb and Zn in  
37 trophosome and vestimentum of the tube worm *Riftia pachyptila* from Guaymas basin, Gulf of California.  
38 *Deep Sea Res I* 2005;7:1319-1323.  
39  
40 Sander SG, Koschinsky A, Massoth G, Stott M, Hunter K. Organic complexation of copper in deep-sea  
41 hydrothermal vent systems. *Environ Chem* 2007;4,81-89.  
42  
43 Sarradin PM, Caprais JC, Briand P, Gaill F, Shillito B, Desbruyères D. Chemical and thermal description of the  
44 Genesis hydrothermal vent community environment (13°N, EPR). *Cah Biol Mar* 1998;159-167.  
45  
46 Sarradin PM, Caprais JC, Riso R, Kerouel R, Aminot A. Chemical environment of the hydrothermal mussels  
47 communities in the Lucky Strike and Menez Gwen vent fields, MAR. *Cah Biol Mar* 1999;93-104.  
48  
49 Sarradin PM, Le Bris N, Le Gall C, Rodier P. Fe analysis by the ferrozine method: Adaptation to FIA towards in  
50 situ analysis in hydrothermal environment. *Talanta* 2005;5:1131-1138.  
51  
52 Sarrazin J, Juniper S K, Massoth G, Legendre P. Physical and Chemical factors influencing species distributions on  
53 hydrothermal sulfide edifices of the Juan de Fuca Ridge, Northeast Pacific. *Mar Ecol Prog Ser* 1999;89-112.  
54  
55 Trefry JH, Trocine RP. Iron and copper enrichment of suspended particles in dispersed hydrothermal plumes along  
56 the mid Atlantic ridge. *Geophys Res Let* 1985;8:506-509.  
57  
58  
59  
60  
61  
62  
63  
64  
65

1  
2  
3  
4  
5  
6  
7  
8  
9  
10  
11  
12  
13  
14  
15  
16  
17  
18  
19  
20  
21  
22  
23  
24  
25  
26  
27  
28  
29  
30  
31  
32  
33  
34  
35  
36  
37  
38  
39  
40  
41  
42  
43  
44  
45  
46  
47  
48  
49  
50  
51  
52  
53  
54  
55  
56  
57  
58  
59  
60  
61  
62  
63  
64  
65

Trocine RP, Trefy JH. Distribution and chemistry of suspended particles from an active hydrothermal vent site on the Mid-Atlantic Ridge at 26°N. *Earth Planet Sci Lett* 1988;1-15.

Truchet M, Ballan-Dufrançais C, Jeantet AY, Lechaire JP, Cosson RP. Le trophosome de *Riftia pachyptila* et *Tevnia jerichonana* (Vestimentifera): bioaccumulations métalliques et métabolismes du soufre. *Cah Biol Mar* 1998;129-141.

Urcuyo IA, Massoth GJ, Julian D, Fisher CR. Habitat, growth and physiological ecology of a basaltic community of *Ridgeia piscesae* from the Juan de Fuca Ridge. *Deep Sea Res I* 2003;763-780.

Von Damm KL. Systematics of and postulated controls on submarine hydrothermal solution chemistry. *J Geophys Res* 1988;B5:4551-4561.

Von Damm KL. Controls on the chemistry and temporal variability of seafloor hydrothermal fluids. *Seafloor Hydrothermal Systems: Physical, Chemical, Biological and Geological Interactions*. SE Humphris, RA Zierenberg, LS Mullineaux, RE Thomson (Eds). Washington, AGU 1995a;91:222, 247.

Von Damm KL, Oostling SE, Kozlowski R, Buttermore LG, Colodner DC, Edmonds HN, Edmond JM, Grebmeler JM. Evolution of East Pacific Rise hydrothermal vent fluids following a volcanic eruption. *Nature* 1995b;47-50.

Von Damm KL, Bray AM, Buttermore LG and Oosting SE. The geochemical controls on vent fluids from the Lucky Strike vent field, Mid Atlantic Ridge. *Earth Planet Sci Lett* 1998;521-536.

Wang W-X. Interactions of trace metals and different marine food chains. *Mar Ecol Prog Ser* 2002;295-309.

Zbinden M, Le Bris N, Compère P, Martinez I, Guyot F, Gaill F. Mineralogical gradients associated with Alvinellids at deep-sea hydrothermal vents. *Deep Sea Res I* 2003;2:269-280.

Fig.1

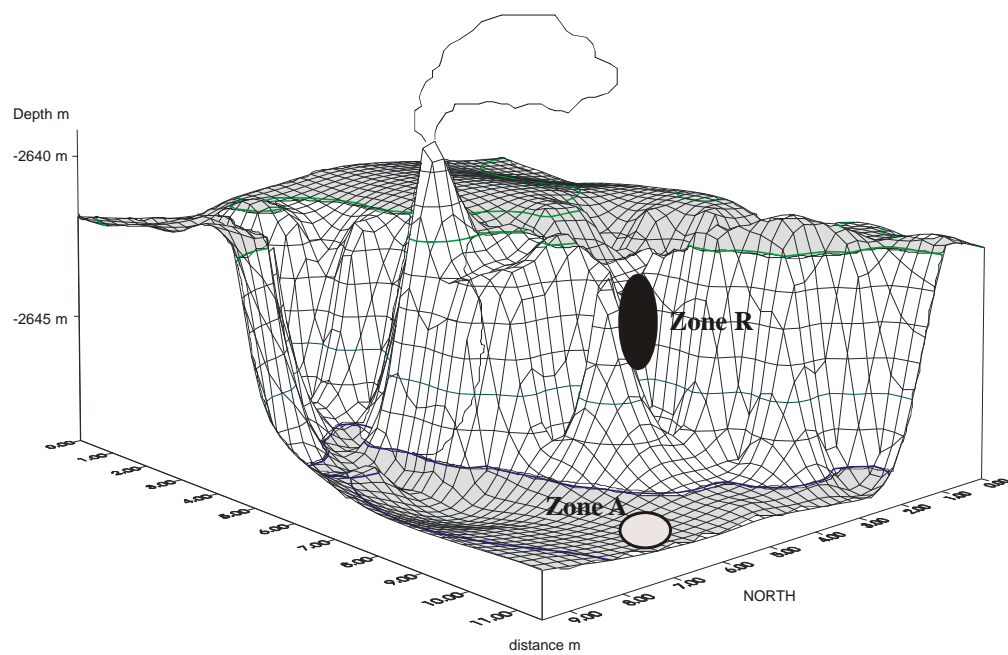


Fig 2

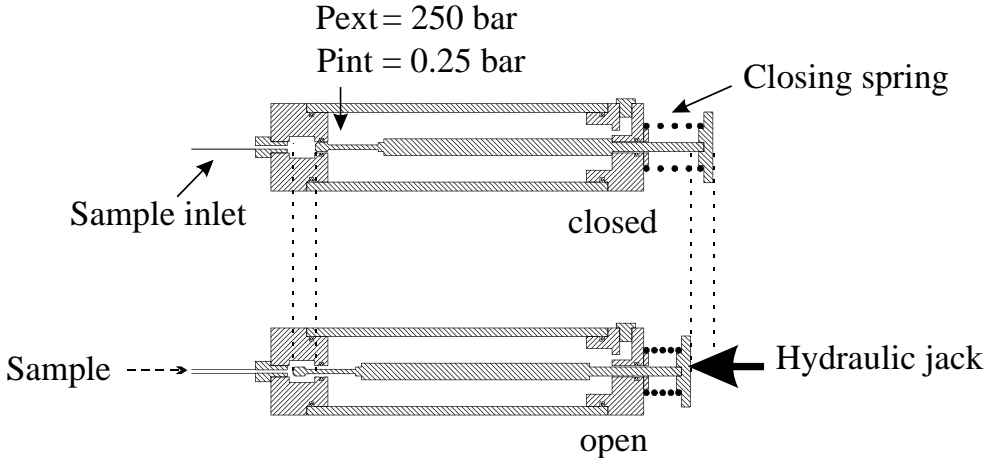


Fig 3

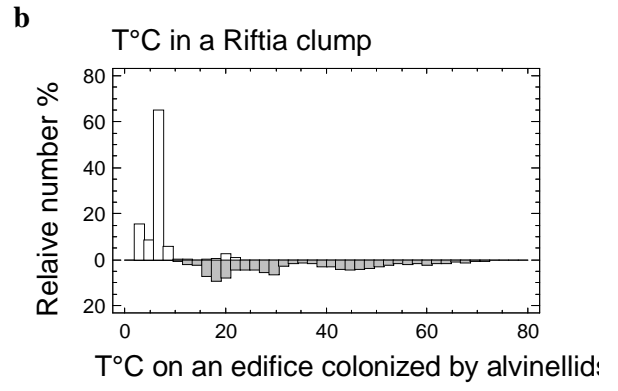
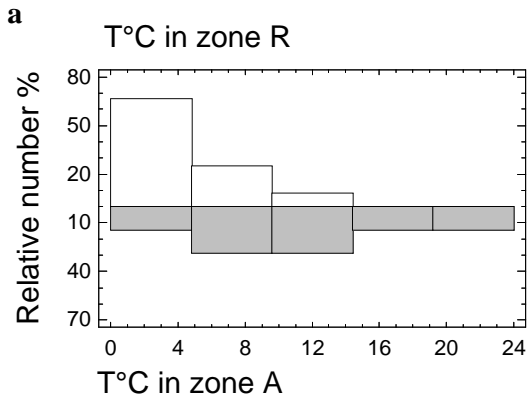


Fig 4

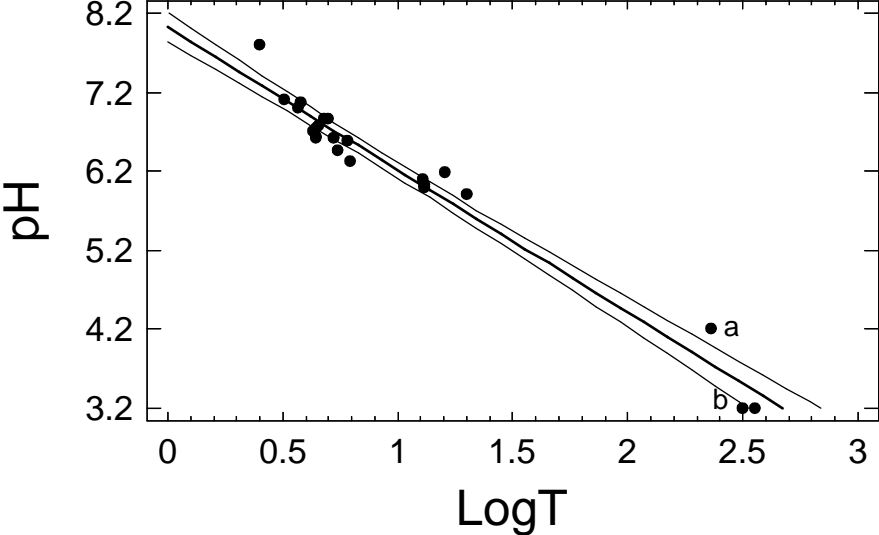


Fig 5

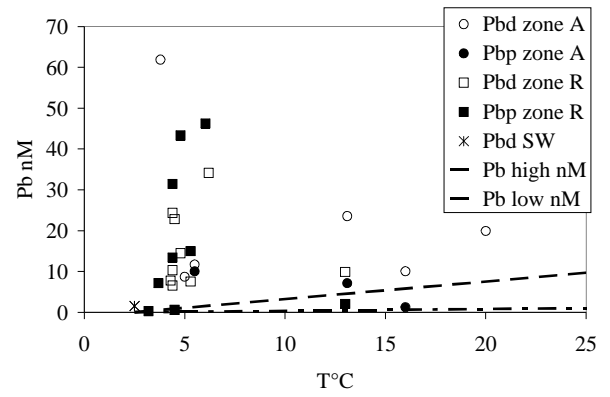
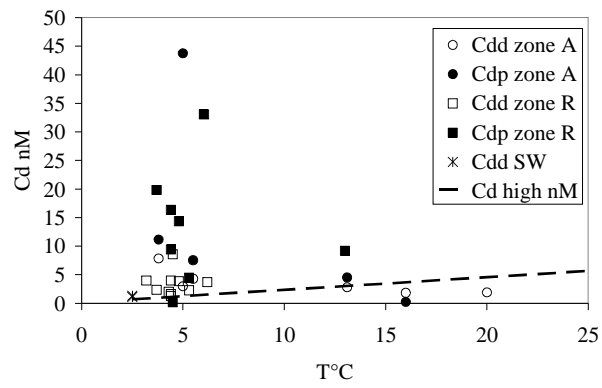
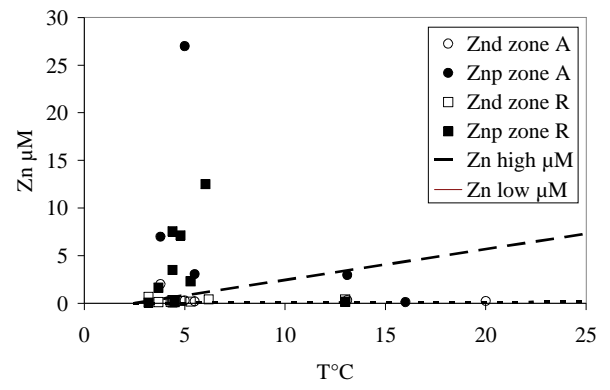
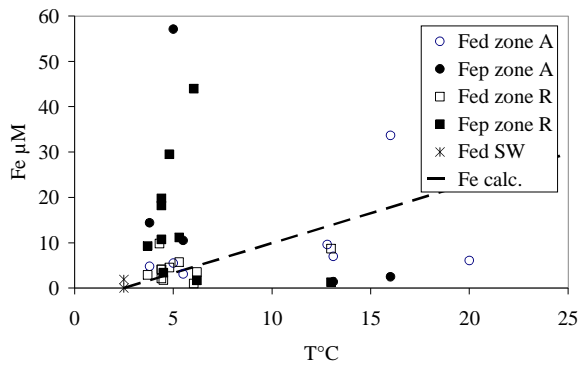


Fig 6:

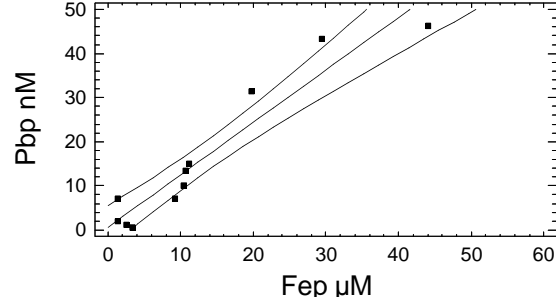
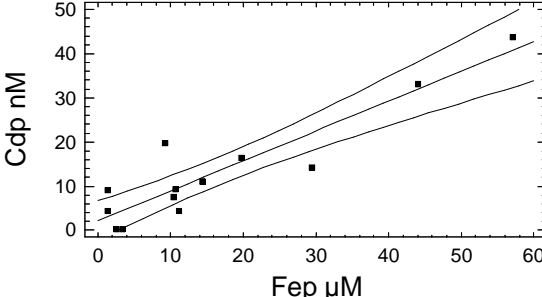
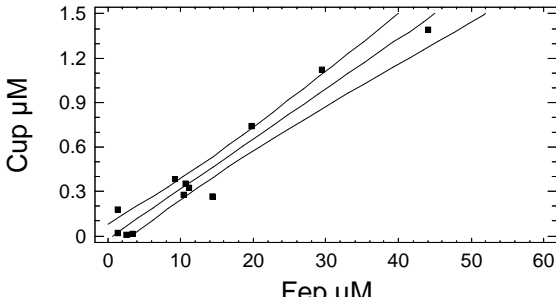
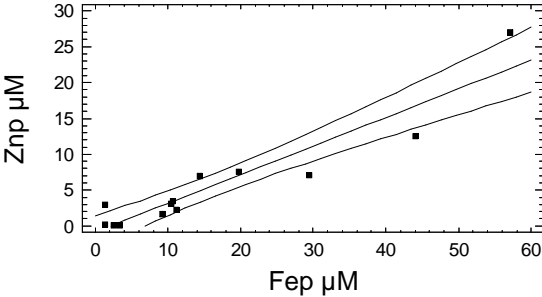
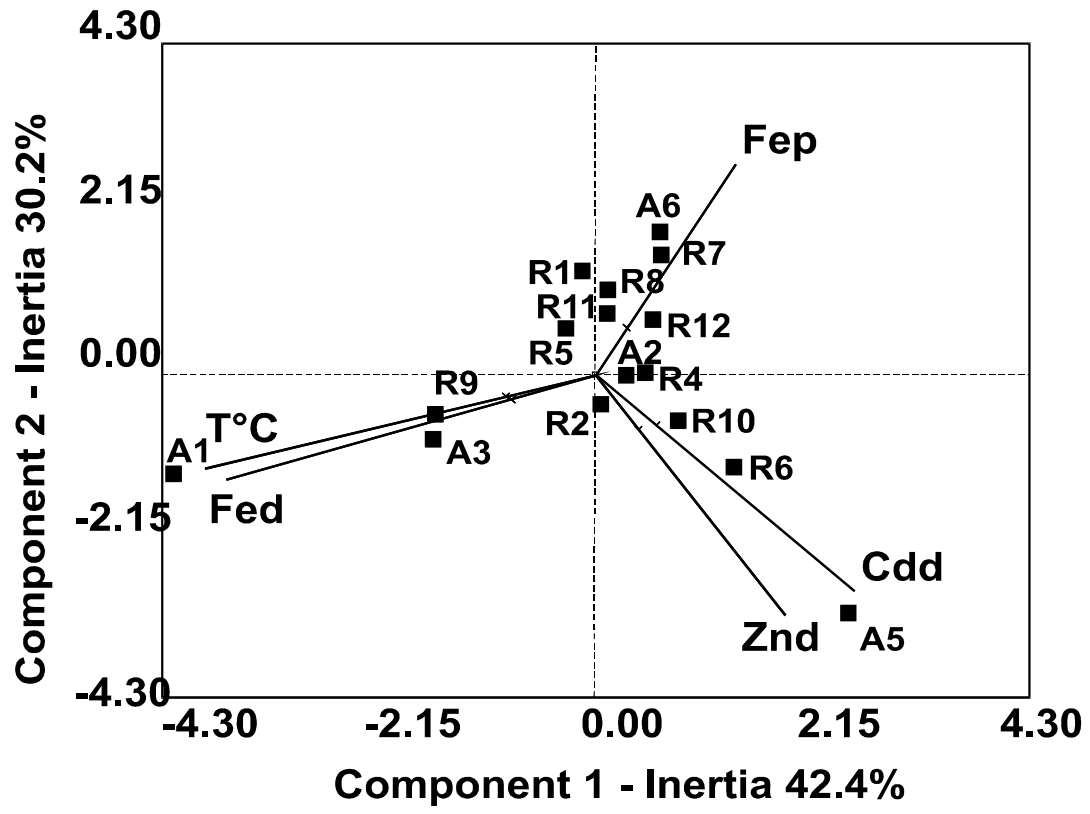


Fig 7



## Figure captions

Fig. 1: 3D schematic representation of the Genesis chimney (from Sarradin et al. 1998). The dark area corresponds to the sampling area “zone R”, the grey one to “zone A”.

Fig. 2: Schematic view of the vacuum based sampling device manipulated and actuated by the hydraulic jack of the submersible. The initial internal pressure is 0.25 bar ( $P_{int}$ ). Temperature is recorded at the extremity of the sample inlet by an autonomous probe. The frit holder is connected to the sample inlet.

Fig 3: a), Distribution of the relative number (%) of temperature measurements of the samples in zones A and R,  $n=19$ . b) Distribution of the relative number (%) of temperature measurements within different microhabitats colonized by *Riftia pachyptila* or by alvinellid worms. This graph was obtained by gathering temperature data measured by autonomous probes (Micrel®) during 2 cruises on the EPR (HOT96 and HOPE99),  $n = 10478$ .

Fig. 4: Log Temperature vs. pH relationship. The dataset is enriched with endmember concentrations from a) Le Bris et al. (2003) and b) Von Damm (1995a).  $R^2 = 96.0\%$ ,  $pH = 8.02 - 1.81 \cdot \text{Log}T$ . The dotted line represents the confidence interval at 95%.

Fig. 5: Dissolved ( $M_d$ ,  $<2\mu\text{m}$ ) and particulate ( $M_p$ ,  $>2\mu\text{m}$ ) metal concentrations vs. temperature compared with theoretical dilution lines. Theoretical dilution lines were calculated from published high and low endmember concentrations simulating a simple dilution of hydrothermal fluid with seawater.

Fig. 6: Particulate metal ( $M_p$ ) vs. particulate Fe ( $F_{ep}$ ) relationship. The correlation coefficients obtained for particulate Zn, Cu, Cd and Pb vs. particulate Fe are respectively 0.939, 0.972, 0.918, 0.957. The dotted line represents the confidence interval at 95%.

Fig. 7: Biplot of components 1-2 extracted from the PCA and explaining 72 % of the variability in the dataset. The samples (square symbols) are marked according to the sampling zone (R for Riftia clumps, A for colony of Alvinellids).

**Table**[Click here to download Table: SarradinTable1-4R2.doc](#)

|        | Cu(nM)       |             | Pb (nM)      |             | Cd (nM)      |             |
|--------|--------------|-------------|--------------|-------------|--------------|-------------|
|        | Certified v. | Measured v. | Certified v. | Measured v. | Certified v. | Measured v. |
| NASS-5 | 4.7±0.7      | 4.4±0.2     | 0.04±0.02    | 0.05±0.02   | 0.20±0.03    | 0.17±0.02   |
| CASS-3 | 8.1±1.0      | 7.6±0.5     | 0.06±0.02    | 0.07±0.01   | 0.27±0.04    | 0.26±0.04   |
| SLEW-2 | 25.7±1.7     | 27.2±1.4    | 0.09±0.01    | 0.08±0.01   | 0.17±0.02    | 0.15±0.02   |

**Table 1:** Analysis of Cu, Pb and Cd in certified seawater samples: NASS-5 oceanic seawater, CASS-3 coastal seawater, SLEW-2 estuarine water. Values (v.) are expressed as mean ± confidence interval (95%)

| Sampling zone | T°C  | pH  | % fluid | Fed $\mu\text{M}$ | Fep $\mu\text{M}$ | Cud $\mu\text{M}$ | Cup $\mu\text{M}$ | Znd $\mu\text{M}$ | Znp $\mu\text{M}$ | Cdd nM | Cdp nM | Pbd nM | Pbp nM |
|---------------|------|-----|---------|-------------------|-------------------|-------------------|-------------------|-------------------|-------------------|--------|--------|--------|--------|
| R1            | 4.4  | 6.6 | 1.1     | 4.1               | 19.8              | 0.18              | 0.742             | 0.07              | 7.54              | 1.62   | 16.34  | 10.29  | 31.43  |
| R2            | 6.2  | 6.3 | 1.9     | 3.5               | 1.7               | 0.40              | nd                | 0.40              | nd                | 3.69   | nd     | 34.13  | nd     |
| R3            | 4.3  | 6.7 | 1.1     | 9.8               | nd                | 0.19              | nd                | 0.13              | nd                | 1.98   | nd     | 7.77   | nd     |
| R4            | 4.4  | 6.6 | 1.1     | 4.1               | 10.7              | 1.13              | 0.353             | 0.30              | 3.49              | 3.96   | 9.41   | 24.32  | 13.39  |
| R5            | 5.3  | 6.6 | 1.5     | 5.7               | 11.2              | 0.22              | 0.325             | 0.16              | 2.30              | 2.25   | 4.47   | 7.52   | 14.94  |
| R6            | 4.5  | 6.8 | 1.1     | 1.8               | 3.4               | 0.49              | 0.016             | 0.21              | 0.09              | 8.56   | 0.20   | 22.82  | 0.56   |
| R7            | 6.0  | 6.6 | 1.8     | 1.0               | 44                | nd                | 1.393             | nd                | 12.50             | nd     | 33.04  | nd     | 46.22  |
| R8            | 4.4  | 6.8 | 1.1     | 2.1               | 18.2              | 0.36              | nd                | 0.32              | nd                | 1.26   | nd     | 6.55   | nd     |
| R9            | 13.1 | 6.0 | 4.9     | 7.0               | 1.4               | 0.44              | 0.177             | 0.32              | 2.95              | 2.79   | 4.51   | 23.54  | 7.12   |
| R10           | 3.2  | 7.1 | 0.6     | nd                | nd                | 0.80              | 0.004             | 0.65              | 0.06              | 3.96   | nd     | nd     | 0.26   |
| R11           | 3.7  | 7.0 | 0.8     | 2.9               | 9.3               | 0.32              | 0.383             | 0.12              | 1.61              | 2.34   | 19.83  | nd     | 7.13   |
| R12           | 4.8  | 6.9 | 1.3     | 4.5               | 29.5              | 0.49              | 1.122             | 0.23              | 7.11              | 3.87   | 14.34  | 14.47  | 43.33  |
| A1            | 16.0 | 6.2 | 6.2     | 33.7              | 2.5               | 0.17              | 0.009             | nd                | 0.11              | 1.80   | 0.24   | 10.05  | 1.20   |
| A2            | 5.5  | 6.5 | 1.6     | 3.1               | 10.5              | 0.24              | 0.280             | 0.21              | 3.06              | 4.28   | 7.52   | 11.70  | 10.03  |
| A3            | 13.0 | 6.0 | 4.9     | 8.7               | 1.3               | 0.23              | 0.018             | 0.40              | 0.15              | nd     | 9.19   | 9.85   | 2.03   |
| A4            | 12.8 | 6.1 | 4.8     | 9.6               | nd                | nd                | nd                | nd                | nd                | nd     | nd     | nd     | nd     |
| A5            | 3.8  | 7.1 | 0.8     | 4.8               | 14.4              | 0.39              | 0.266             | 2.00              | 6.98              | 7.84   | 11.15  | 61.89  | 81.30  |
| A6            | 5.0  | 6.9 | 1.4     | 5.5               | 57.1              | 0.34              | 0.873             | 0.29              | 27.00             | 2.97   | 43.7   | 8.69   | 251.53 |
| A7            | 20.0 | 5.9 | 7.9     | 6.1               | nd                | nd                | nd                | 0.23              | nd                | 1.89   | nd     | 19.90  | nd     |
| SW1           | 1.9  | 7.6 | 0.0     | 1.9               | nd                | 0.02              | nd                | nd                | nd                | 1.1    | nd     | 1.5    | nd     |
| SW2           | nd   | 7.6 | nd      | <LD               | nd                | 0.01              | nd                | nd                | nd                | 1.3    | nd     | 1.5    | nd     |

**Table 2:** Temperature, pH and metal concentrations measured in the water samples. d refers to dissolved concentration, i.e. not retained on a 2 $\mu\text{m}$  frit, p refers to particulate concentration, i.e. retained on a 2 $\mu\text{m}$  frit. The frits corresponding to samples R3 and A4 were used for the MEB studies. Samples SW1 and SW2 were taken ca. 500 meters away from the active area. % fluid is an estimation of the content of hydrothermal fluid in mixed with seawater (see § 3-3).

nd : not determined, <LD lower than the detection limit.

|                                  | References  | T°C     | Fe (µM)   | Cu (µM)   | Zn (µM)   | Cd (nM)  | Pb (nM)  |
|----------------------------------|---|---------|-----------|-----------|-----------|----------|----------|
| <b>Endmember, 13°N</b>           | Cosson (1996), Von Damm (1995a), Le Bris et al. (2003)                | 230-359 | 600-10800 |           | 2-102     | 55-70    | 14-135   |
| <b>Surrounding organisms</b>     |   |         |           |           |           |          |          |
| EPR, 13°N                        | This study * R, A   | 3.8-20  | 5.2-62.6  | 0.18-1.6  | 0.3-27.3  | 2.0-46.7 | 11-260   |
| EPR, 13°N                        | Desbruyères et al. (1998) A   |         |           | 1.38-3.27 |           | 16-133   |          |
| EPR, 9°N                         | Di Meo-Savoie et al. (2004) A   | 7.5-40  | 72-730    | 0.08-1.94 | 2.9-41.3  | 2.8-33   | 20-520   |
| Mid Atlantic Ridge               | Geret et al. (1998) Sarradin et al. (1999), Geret et al. (2002), M, S | 4.7-25  | 58-1470   | 0.02-3.2  |           |          | 0.96-120 |
| Mid Atlantic Ridge               | Kadar et al. (2005) M, S  | 4.3-8   | 3.8-10.3  | 0.5-1.99  | 0.25-1.64 |          | 1.6-20   |
| <b>North Pacific deep waters</b> | Donat and Bruland (1995)  |         | 0.001     | 0.005     | 0.008     | 1        | 0.005    |

**Table 3:** Temperature and composition of endmember vent fluids from 13°N, EPR, diluted fluids surrounding hydrothermal organisms and North Pacific deep waters.

\* Total metal concentration (dissolved + particulate).

R: *Riftia pachyptila* clump, A: colony of alvinellids, M: mussel bed, S: shrimps

| Structure                | Composition       | Size $\mu\text{m}$ | n  | Comment  |
|--------------------------|-------------------|--------------------|----|--|
| Wurtzite                 | ZnFeS             | 1-10/50            | 9  | hexagonal, individual or stacked crystals          |
| Collomorphous (wurtzite) | ZnFeS             | 20                 | 5  | spheres, stacked                                   |
| Sphalerite               | ZnS/ ZnFeS        | 15                 | 2  | crystal + stacked                                  |
| Pyrite                   | FeS <sub>2</sub>  | 20                 | 3  | cubic  |
| Collomorphous (pyrite)   | FeS <sub>2</sub>  | 5-20               | 5  | sphere, stacked                                    |
| Sulfur                   | S                 | 2-5                | 1  | globule, stacked                                   |
| Anhydrite                | CaSO <sub>4</sub> | 60                 | 1  | not eroded crystal                                 |
| "Biofilm"                |                   |                    | 32 | microcrystalline assemblage associated to biofilms |
| Organic fragments        |                   |                    | 4  |  |

**Table 4:** Mineralogical composition of the particles, n is the number of observations for a total of 32.

Sarradin  
STOTEN-D-07-00750R1

We have followed all the reviewer's comments. Our modification start with a < in the following text

Reviewers' comments:

2. Unclear relationship between observed metal data and faunal association with the microhabitats; While I have no concern about using PCA for a statistical evaluation of the data, I am still not completely satisfied with the discussion and conclusion from the statistical results. It would be nice to have some concluding sentences about the different metal composition of the two microhabitats and possible explanations, why tubeworms may favor this environment and the alvinellid worms the other. Does the limited variability in area R indicate a more homogeneous microenvironment (and possibly lower tolerance limits for metals) of the tubeworms, and the higher variability of the values in area A that the alvinellid worms are exposed to stronger metal gradients and/or fluctuations than the tubeworms?

<Concluding sentences have been added to section 3.5

Riftia clumps are present in zone R characterized by a limited variability, low temperature and metal concentrations whereas Alvinellids worms in zone A are exposed to stronger metal gradients and fluctuations than the tubeworms. This distribution along the chemical gradient can be linked both to the availability of energy sources but also to the ability of Riftia pachyptila or alvinellids worms to sustain the metallic load, alvinellids being potentially more adapted to tolerate harsher conditions. The possible metal entry routes may also be different as only the dissolved metal fraction will be available for R. pachyptila, whereas both dissolved and particulate fractions will be available for alvinellid worms.

I also have a few specific comments:

Page 1, Line 39, 40, abstract: I doubt that coprecipitation with Fe is the correct expression for the formation of the listed mineral phases. Wurtzite, sphalerite and pyrite are discrete phases that precipitate from hydrothermal solutions, as well as Cu-bearing phases such as chalcopyrite.

< co precipitation has been replaced throughtout the text by precipitation

Page 1, Line 42,43: Say how the distribution of the fauna is related to the gradients.

<added in the text

The distribution of the dominant observed fauna has been related to the gradient resulting from the dilution process, with the alvinellids worms colonizing the hotter and more variable part of the mixing zone, but also to the metallic load of the mixing zone.

Page 3, Line 50: What is PSA?

<added in the text potentiometric stripping analysis

Page 4, Lines 28-29: Fed, Cud etc. need to be defined somewhere in the text. I would suggest to make the d for "dissolved" subscript.

< done in the text

The concentrations of dissolved metals obtained in sample SW1 (Fe < detection limit, Cu 0.01  $\mu$ M, Cd 1.3 nM, Pb 1.5 nM) are close to those currently reported for North Pacific deep waters (Fe 0.01  $\mu$ M, Cu 0.005  $\mu$ M, Cd 1 nM, Pb 0.005 nM, Donat and Bruland, 1995) except for Pb.

Page 6, lines 4-18. Is the temperature really a conservative parameter? Has the calculation of the fluid percentage been checked with the endmember data of a conservative element? Comparative calculations by Koschinsky et al. (Geochimica et Cosmochimica Acta 66, 1409-1427) had shown that conservative elements such as Li and Rb are better parameters for endmember calculations than

temperature, because conductive cooling in the subsurface can make temperature behave non-conservative during mixing.

< a sentence has been added in the text

This result confirms that at the scale and in the range studied, pH and temperature can be assumed to follow a semi-conservative process and can be used as tracers of the dilution, even though conductive cooling in the subsurface can modify its conservative behavior during mixing.

Page 7, line 40: Cu sulfide is a typical high-temperature precipitate, and not something that forms in the cold part of the chimneys.

< deleted in the text

Line 58: delete one "settle"

<done

Page 8, line 17: correct "calchophile" to "chalcophile"

<done

Figure 5: Legends of the Zn and Pb graphs: what does "Zn high  $\mu\text{M}$ , Zn low  $\mu\text{M}$ , etc. mean?

< done in the legend

Figure caption, figure 6: Include "(Fep)" after "particulate Fe"

< done